Comparison of the new simulation setup used in the accompanying article (S-new) to the evaluation simulations (S1/S2) published by Jöckel et al. (2006)

A. Kerkweg &

P. Jöckel & A. Pozzer & H. Tost &

R. Sander & J. Lelieveld

Air Chemistry Department
Max-Planck Institute of Chemistry
PO Box 3060, 55020 Mainz, Germany
akerkweg@mpch-mainz.mpg.de

This document is part of the electronic supplement of our article "Consistent simulation of bromine chemistry from the marine boundary layer to the stratosphere: Part-I: Model description, sea salt aerosols and pH" in Atmos. Chem. Phys. Discuss. (2008), available at: http://www.atmos-chem-phys.org

Date: February 22, 2008

1 Introduction

For the simulations of bromine chemistry the model setup was changed compared to Jöckel et al. (2006). One difference is the vertical model resolution. Instead of 90 vertical layers 87 vertical layers are used. The 87 layer setup resolves the boundary layer and the lower troposphere much better than the L90 setup, as is illustrated in Figure 0. The red lines depict the L87, the black lines the L90 setup. Note: this Figure is number "0" as this is an additional figure and the following figure numbers correspond to the respective figure numbers in Jöckel et al. (2006).

To be sure that the new model configuration still provides results comparable to the extensively evaluated earlier setup, we reproduced the figures of Jöckel et al. (2006). The results will be shown in the following.

F. 1 Figure 1 of Jöckel et al. (2006) is a diagram of the coupling between the submodels. The number of submodels is larger in the new simulation. But as all new submodels are of diagnostic nature no additional coupling among the tracers and between other submodels is introduced.

F. 2 Figure 2 of Jöckel et al. (2006) displays the quasi-biennial oscillation which was consistently simulated within the S1/S2 simulations. Since we are in the present study not primarily interested in showing that the QBO is developing in the model by itself, it was forced by the MESSy submodel QBO to yield the observed QBO phase. Therefore our simulation matches the observations better than the simulations by Jöckel et al. (2006).

F. 3 In contrast to the S1 simulation, instead of 8 years only 3 years (1998-2000) are analysed. Nevertheless, the correlations between the simulated temperatures in S-new and the HALOE measurements are very similar or even higher as for S1.

F. 4 The original figure of Jöckel et al. (2006) depicts results for the year 2003 as for this year MIPAS data is available enabling a comparison with observations. Since the S-new simulation covers only the years 1998-2000, this comparison is not possible. Instead figures for the year 2000 for the S1 and the S-new simulation are shown. The results are very similar. Only the reduced cold biases in the S1/S2 simulations are larger again in S-new. This might be due to the coarser resolution of the current model setup (L87MA) in this altitude region in contrast to the relatively high resolution in the L90MA setup.

F. 5 Again results for the year 2000 are shown for both simulations. The figures are almost identical for S1 and S-new; thus the conclusions of Jöckel et al. (2006) are also valid for S-new.

F. 6 In contrast to Fig. 3, the correlations for CH_4 are slightly lower than in the S1 simulation.

F. 7 This figure shows the polar vortex split. This phenomenon only occurred in the year 2002. As the S-new simulation only covers the years 1998-2000, an adequate figure can not be presented here.

F. 8 Same as Figure 7.

F. 9 Figure 9 clearly shows that the S-new simulation also reproduces the inter-annual and seasonal variability of the observed total ozone. Compared to the S1/S2 simulations S-new ozone is substantially lower at mid-latitudes. As in S1/S2 ozone was overestimated in this region, S-new matches better the observations than S1/S2. At high-latitudes the simulations do not differ significantly.

F. 10 The production of ozone in the S-new simulation looks very similar compared to S1. The maximum between 10 and 1 hPa is slightly smaller, which is most likely due to minor changes in the dynamics associated with the lower vertical grid resolution in S-new.

Tabs The ozone budgets of the troposphere (Table 2) and the stratosphere (Table 1) are shown.

In the troposphere the sum of all chemical production terms is larger than in Jöckel et al. (2006), whereas the chemical sinks are smaller or equal in amount. The sinks due to dry deposition differ only slightly in both simulations. The burdens of ozone as well as of stratospheric ozone in the troposphere $O_3^{(s)}$ are approximately 5% larger in our simulation, whereas the inferred stratosphere-to-troposphere (STT) flux is slightly smaller.

In both hemispheres the stratospheric production of ozone is smaller in our simulation compared to Jöckel et al. (2006), but the loss terms are —except for reaction with hydrogen— larger. However, the production and losses are of comparable magnitude. The net production in the northern hemisphere is larger in our simulation by about 10%, whereas the net production in the southern hemisphere is larger in the simulation of Jöckel et al. (2006).

F. 11 At most of the stations the two simulations are very similar. At some locations the S-new simulation is closer to the observations (IZO,KZM,MLO) which is most likely a result of the higher resolution of the boundary layer in the S-new simulation.

F. 12 This comparison with MOPITT data is for the year 2003. This period is not covered in S-new, thus we cannot show a corresponding figure.

F. 13 As the surface NO_x distribution is mainly determined by emissions, which are the same in S1/S2

and S-new, Figure 13 is nearly equal to Figure 13 of Jöckel et al. (2006).

F. 14 Surface HNO_3 is also mainly determined by emissions, thus all statements of Jöckel et al. (2006) also apply for the model setup S-new.

F. 15 In Figure 15 a direct comparison of three different simulations is given. The blue line is the S1 simulation of Jöckel et al. (2006), the green line is the S-new simulation and the red line is the S-hal simulation, discussed in the main article. For NO (upper row) no differences between the green and the blue lines are visible. The profiles of HNO_3 are also very similar. Only for PEM-Tropics-A, DC8, Christmas Island and TRACE-P, DC8, Hawaii, differences can be seen. In these cases the S-new simulation matches the observations slightly better than S1. For PAN again only very small differences are present. Nevertheless, for PAN the observations are better reproduced by the S1 simulation. Note that an update of the higher hydrocarbon chemistry is in progress, which substanially improves the PAN simulation (D. Taraborelli et al., in preparation).

F. 16 Figure 16 shows the OH concentration in the lowest model layer. This is similar to the S1 simulation, only the maximum over south India is slightly lower than in S1.

F. 17 On the one hand the maxima of surface OH in MAM and JJA are lower in S-new (2000) than in S1 (2000-2004 average), on the other hand for all seasons the maxima between 200 and 100 hPa are higher in S-new.

F. 18 Except for Hilo, the ozone profiles are virtually the same in both simulations. For Hilo the ozone profile is better matched in the S1 simulation.

F. 19 There are only very small differences for the seasonal cycles of ozone for the Logan (1999) sites at 400 hPa. Where differences exist, the S-new simulation matches the observations slightly better.

F. 20 Because the comparison with the SHADOZ database is performed exactly on the pressure levels of the model and since the S-new simulation uses a different vertical grid, no 400 hPa level but only a 421 hPa level is available for comparison. we do not interpolate to the 400 hPa level to avoid additional uncertainties. At most locations the S-new simulation matches the observations over the year slightly better.

F. 21 There is no significant difference between both Taylor diagrams comparing the Logan (1999) data with the simulations. In the northern mid-latitudes the correlation of the S-new simulation with the observations is higher compared to S1. In contrast, the southern high-latitudes are higher correlated in S1.

F. 22 The comparison with the SHADOZ database does not reveal a clear picture. Overall the spread of the data points is higher for the S-new simulation.

F. 23 Again, the Figures of Jöckel et al. (2006) are provided for a period which was not covered by the S-new simulation. For comparison we show here the DJF and SON figures for the year 2000 for the S-new (left) and the S1 simulation.

For DJF the figures look very similar. Only at northern high latitudes ozone is lower by approximately 1 µmol/mol compared to the S1 simulation. Since this is a region where the model overestimated the observations, we conclude that the S-new simulation better reproduces the observations. For SON the maximum is more pronounced and symmetric to the equator in the S-new simulation. The S2 simulation already overestimated ozone in this region, thus S-new overestimates ozone in the northern tropics at $\approx$ 10 hPa even more strongly.

F. 24 At the maxima the HNO_3 mixing ratios are higher by $\approx$ 2 nmol/mol. For SON this is an imporvement compared to S1.

F. 25 Figure 25 in Jöckel et al. (2006) is for 22 September 2002, during the southern hemispheric vortex split, for which data from the MIPAS instrument are available for comparison. Since we cannot show pictures for this point in time for S-new, we rather show a comparison between S1 and S-new for September 22, 2000.

Some minor differences are apparent. Especially the maxima are always silghtly higher in S1 compared to S-new.

F. 26 No significant differences between S-new and S1 are found for the vertical ozone profiles of Logan (1999).

F. 27 The comparison with the vertical ozone profiles of the SHADOZ database in January at all sites shows that the ozone mixing ratio is lower at the tropopause in the S-new simulation compared to S1. The observed ozone profiles are better matched by the S1 simulation.

F. 28 The correlations are equal up to the third digit. Hence both simulations fit the observations very well.

F. 29 The seasonal cycles of ozone for the selected Logan (1999) sites are very similar in both simulations.

F. 30 Both simulations show a high correlation with the observations. The standard deviation is slightly smaller in the S1 simulation.

F. 31 At 40 hPa the S1 simulation matches the observations better than the S-new simulation for all sites, most likely due to the higher resolution of the S1 simulation in the stratosphere.

References

Emmons, L. K., Hauglustaine, D. A., Muller, J.-F., Carroll, M. A., Brasseur, G. P., Brunner, D., Staehelin, J., Thouret, V., and Marenco, A.: Data composites of airborne observation of tropospheric ozone and its precursor, J. Geophys. Res., 105, 20 497–20 538, 2000.

Jöckel, P., Tost, H., Pozzer, A., Brühl, C., Buchholz, J., Ganzeveld, L., Hoor, P., Kerkweg, A., Lawrence, M. G., Sander, R., Steil, B., Stiller, G., Tanarhte, M., Taraborrelli, D., van Aardenne, J., and Lelieveld, J.: The atmospheric chemistry general circulation model ECHAM5/MESSy1: Consistent simulation of ozone from the surface to the mesosphere, Atmos. Chem. Phys., 6, 5067–5104, 2006.

Logan, J. A.: An analysis of ozone-sonde data for the troposphere: Recommendations for testing 3-D models and development of gridded climatology for tropospheric ozone, J. Geophys. Res., 104, 16 115–16 149, 1999.

Table 2: Annual tropospheric ozone budget (S-new simulation) in Tg for the year 2000. RO_2 comprises $C_2H_5O_2$, $CH_3C(O)OO$, $C_3H_7O_2$, $CH_3CH(O_2)CH_2OH$, $CH_3COCH_2O_2$, $C_4H_9O_2$, and peroxy radicals resulting from the oxidation of MVK, MEK and isoprene. Values are rounded to Tg.

	NH	SH	Global
$NO+HO_2$	1992	1338	3330
$NO+RO_2$	399	200	599
$NO+CH_3O_2$	678	456	1134
P	3069	1994	5063
O_3+OH	-325	-236	-561
O_3+HO_2	-843	-575	-1418
$H_2O+O(^1D)$	-1392	-1074	-2466
L	-2560	-1885	-4445
net	509	109	618
dry deposition	-516	-276	-792
change in burden	-8	-1	-9
STT[a]	-1	166	165
burden	182	159	341
STT of $O_3^{(s)}$	644	499	1143
burden of $O_3^{(s)}$	78	63	141

Table 1: Annual stratospheric (tropopause at 10 hPa) ozone budget (S-new simulation; production P, loss L) in Tg for the year 2000. Values are rounded to Tg. The loss terms refer to the catalytic cycles involving families of reactive species.

	NH	SH	Global
P	6256	6253	12509
L, odd oxygen	-527	-547	-1074
L, odd nitrogen	-3267	-3256	-6523
L, odd hydrogen	-1329	-1324	-2653
L, chlorine	-533	-624	-1157
L, bromine	-73	-110	-183
P_{net}	527	392	919

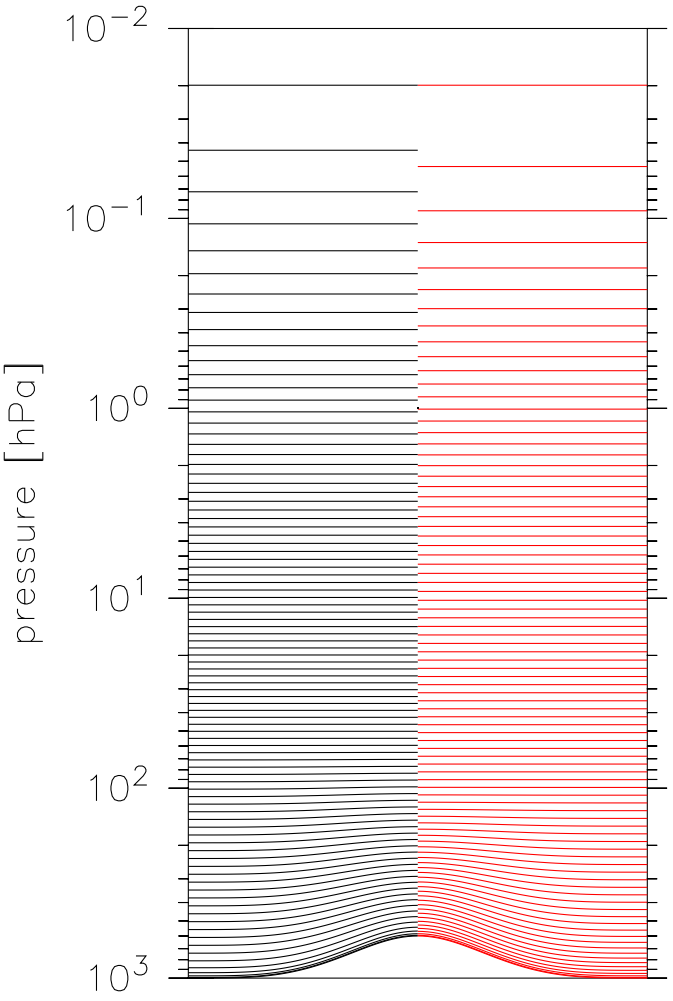

Figure 0: Vertical level structure of the two vertical ECHAM5 resolutions L90 (black) and L87 (red). The lines indicate the level boundaries. An artificial topography was included two show the form of the hybrid pressure levels over elevated terrain.

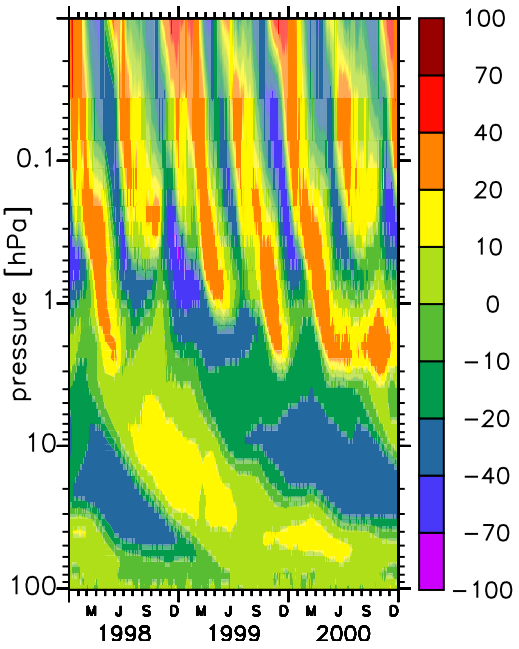

Figure 2: Tropical zonal wind average (in m/s) between 2° S and 2° N and its quasi-biennial oscillation (S-new).

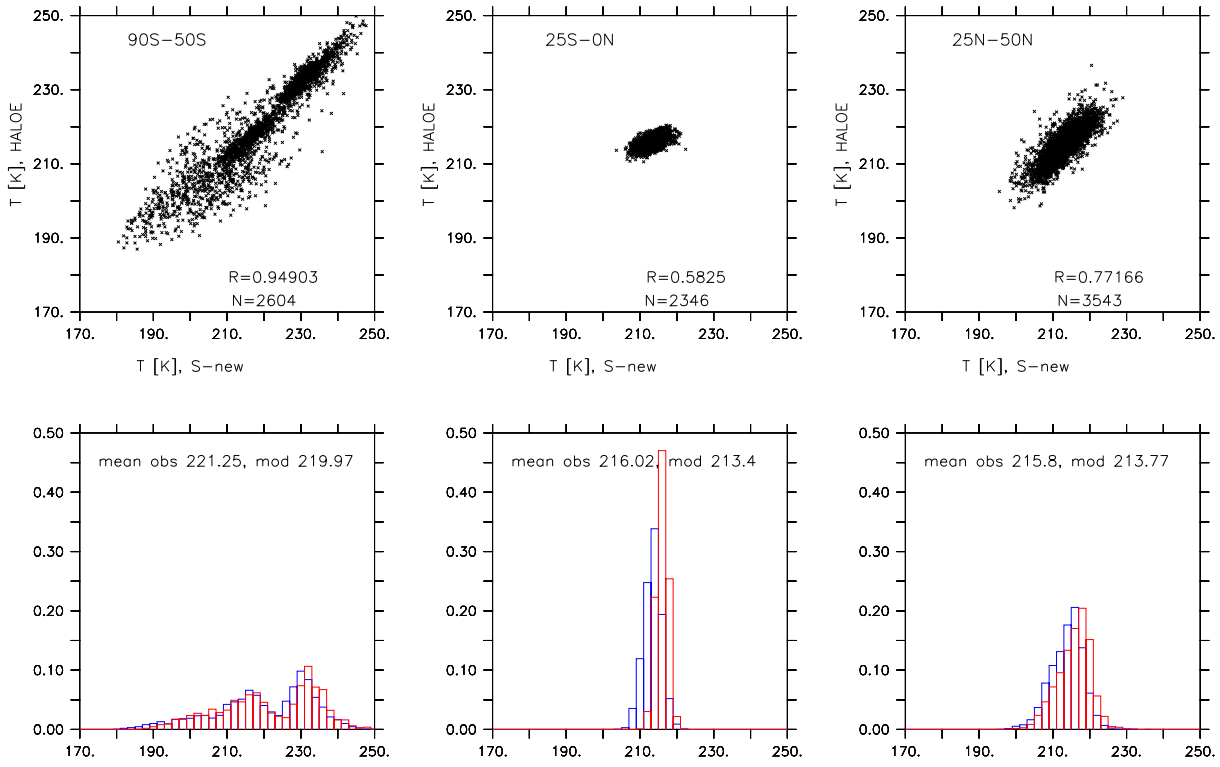

Figure 3: Point-to point comparison of simulated (S-new) temperature with HALOE-data from February 1998 to December 2000 at 30 hPa. The upper panels show the correlations, the lower panels the probability density functions (model: blue; HALOE: red).

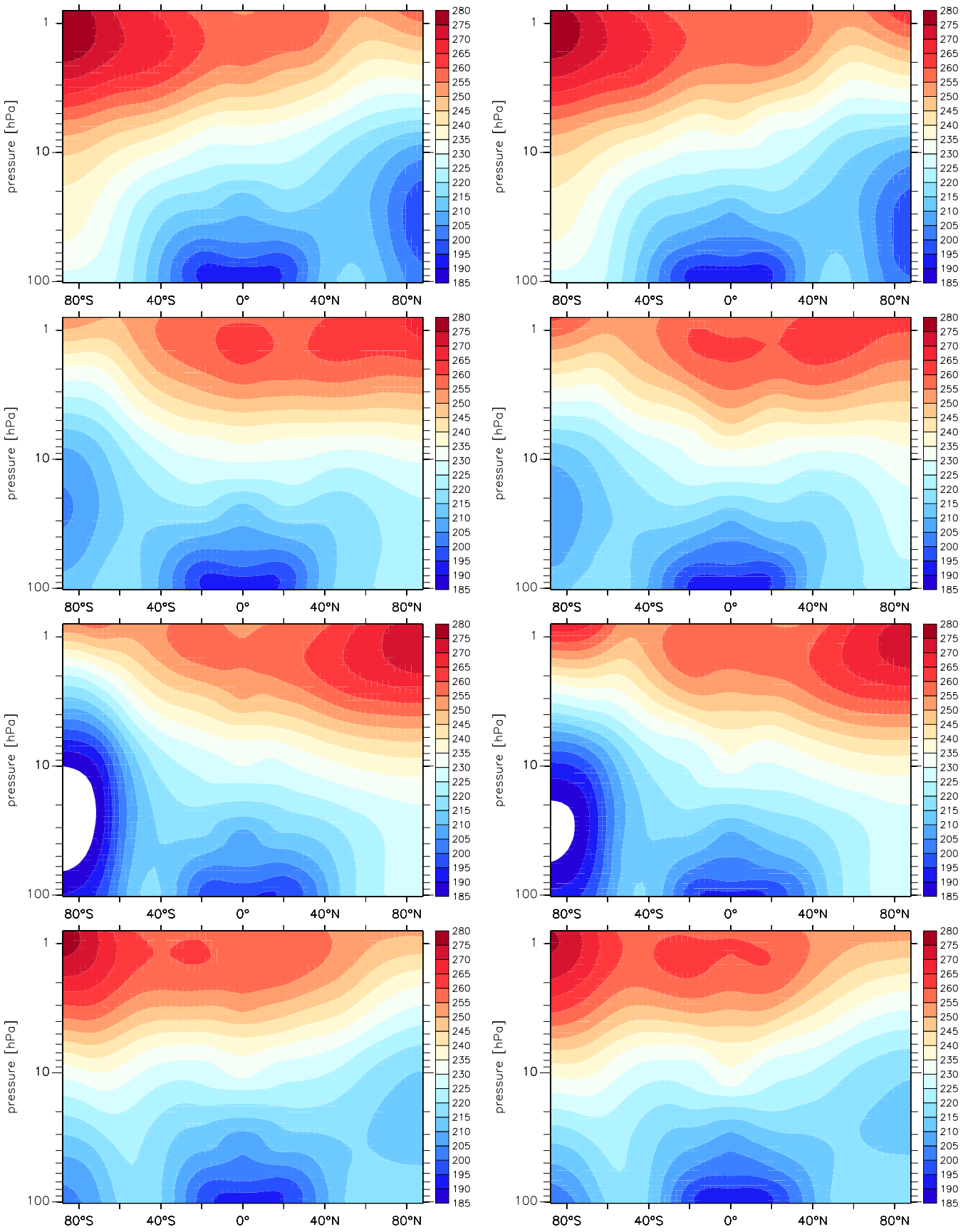

Figure 4: Zonally averaged temperature (in K) from the S-new (left) and the S1 simulation (right). The seasons are DJF (1999/2000), MAM, JJA, and SON (2000) from top to bottom.

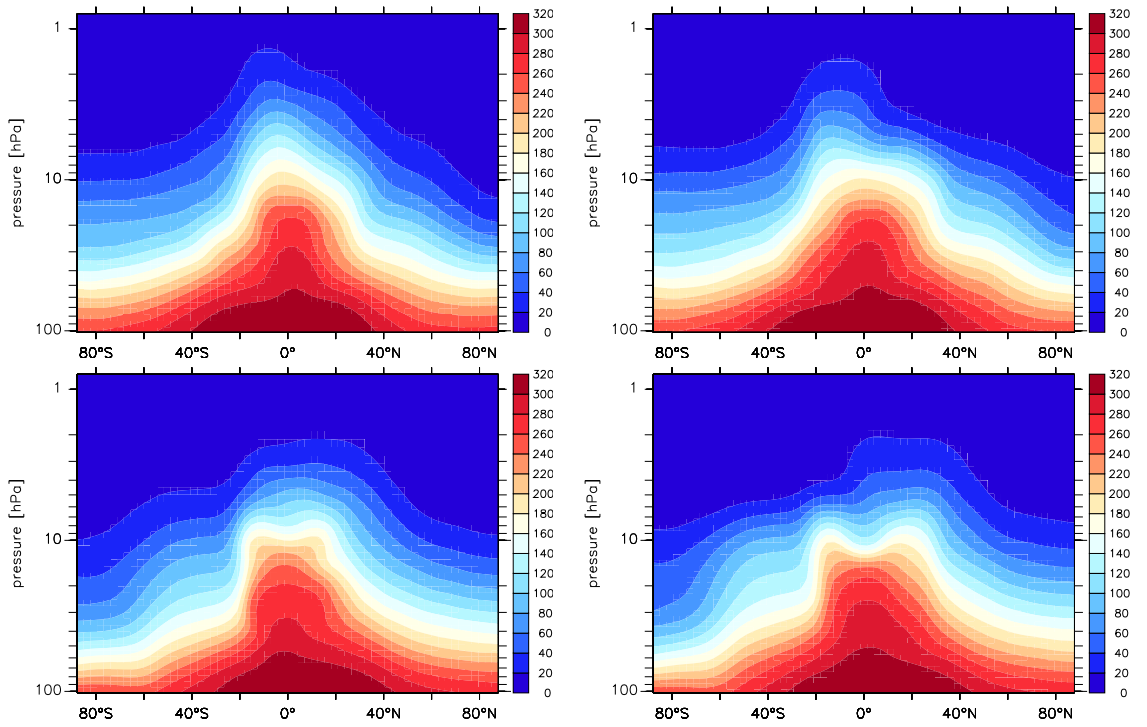

Figure 5: Zonally averaged simulated nitrous oxide (N_2O). Left: S-new; right: S1; top: DJF; bottom: SON (2000)

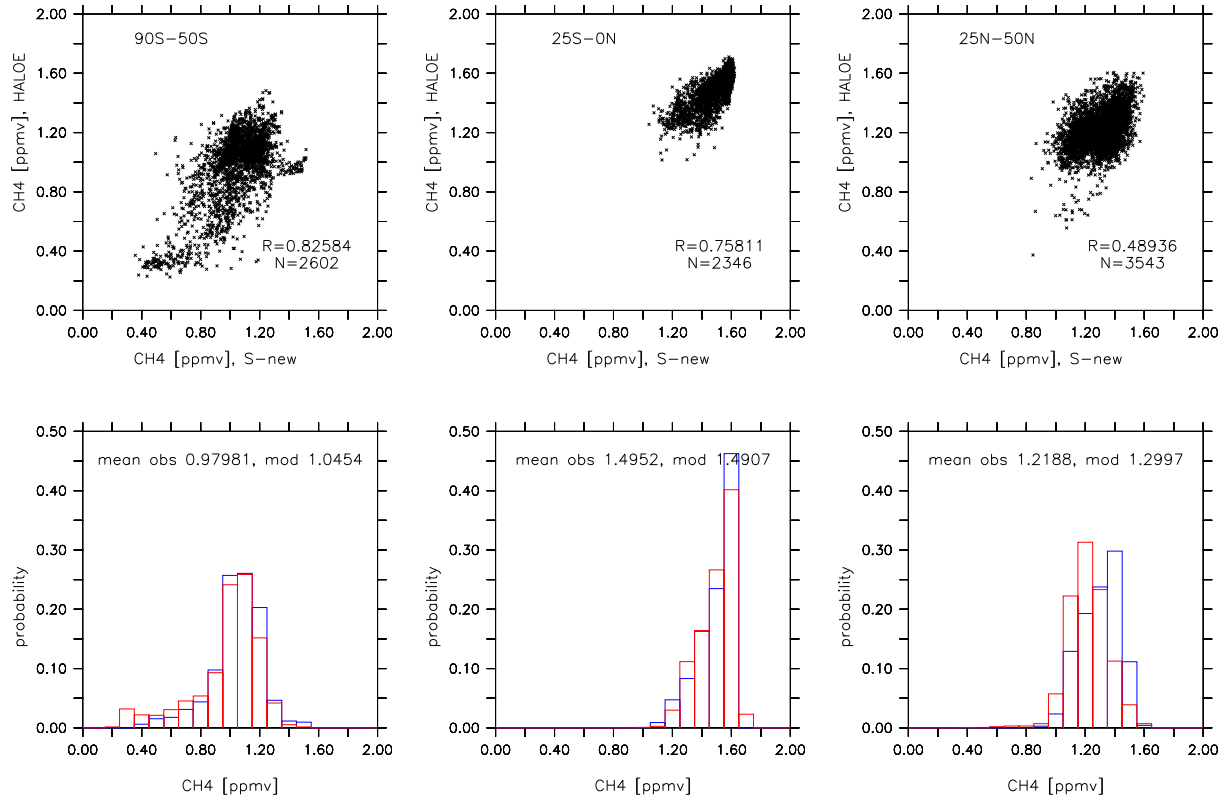

Figure 6: Point-to-point comparison of simulated (S-new) methane (CH_4) with HALOE-data from February 1998 to December 2000 at 30 hPa. The upper panels show the correlations, the lower panels display the probability density functions (model: blue; HALOE: red).

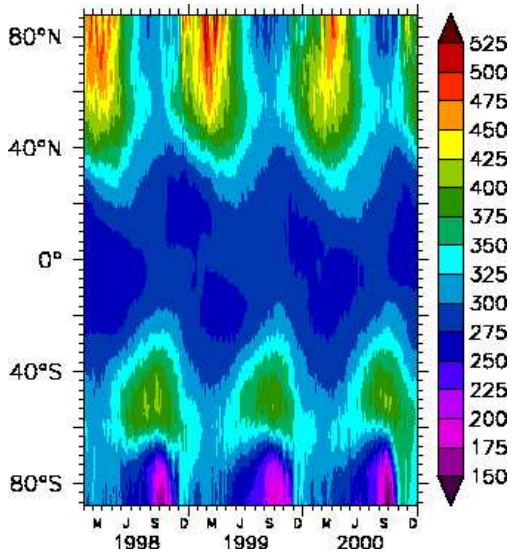

Figure 9: Zonally averaged total ozone (DU) for S-new.

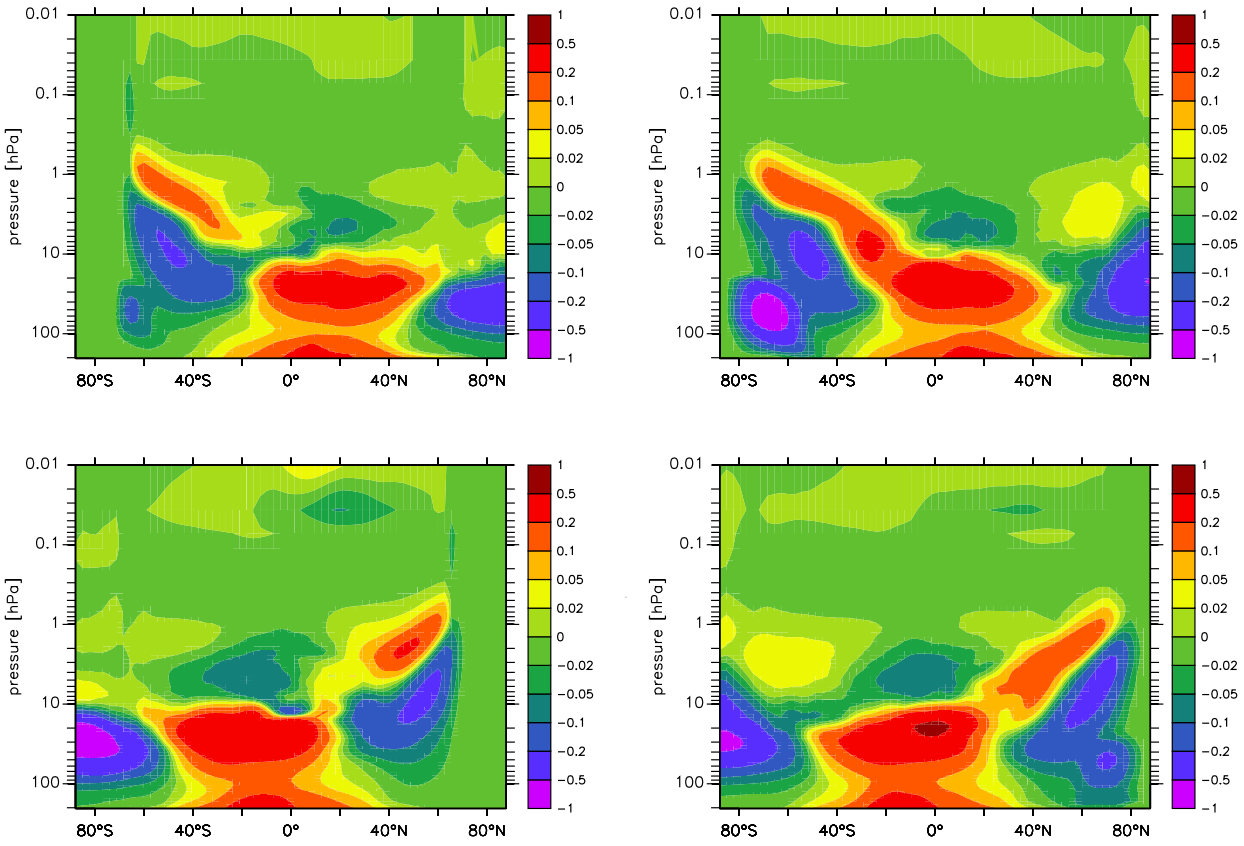

Figure 10: Net chemical ozone production ($P_{net} = P - L$) with P being the chemical production from photolysis of molecular oxygen and L being the chemical loss due to the different catalytic cycles (odd nitrogen, oxygen, chlorine, bromine and hydrogen); June (upper left), August (upper right), December (lower left), and February (lower right). Shown are monthly averages for the year 2000 (S-new) in 10^6 molecules/cm^3/s.

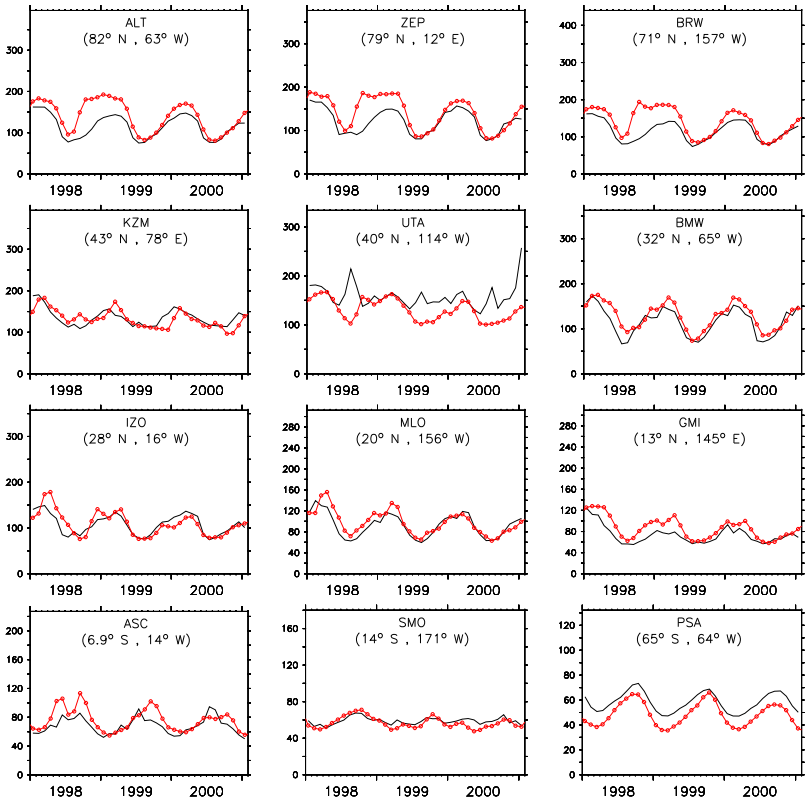

Figure 11: Comparison of simulated (S-new: black line) and observed (red line + dots) CO mixing ratios (in nmol/mol) for selected NOAA/GMD sites (from north to south).

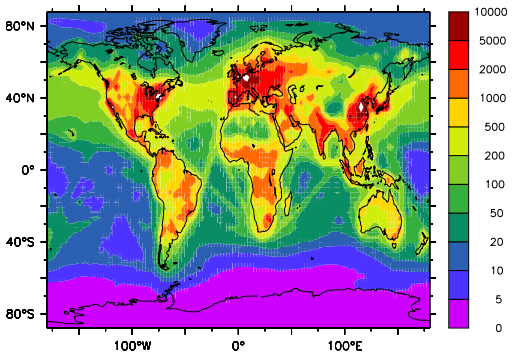

Figure 13: Simulated (S-new) 1-year mean (2000) surface NO_x (=NO_2 + NO) distribution (pmol/mol).

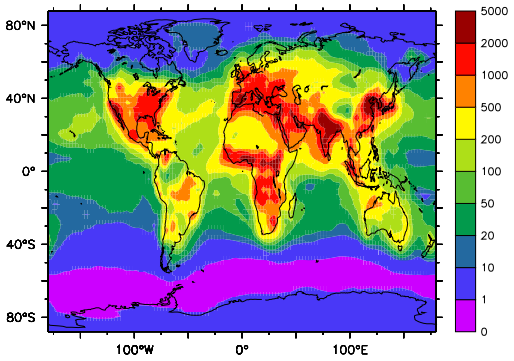

Figure 14: Simulated (S-new) 1-year mean (2000) surface HNO_3 distribution (pmol/mol).

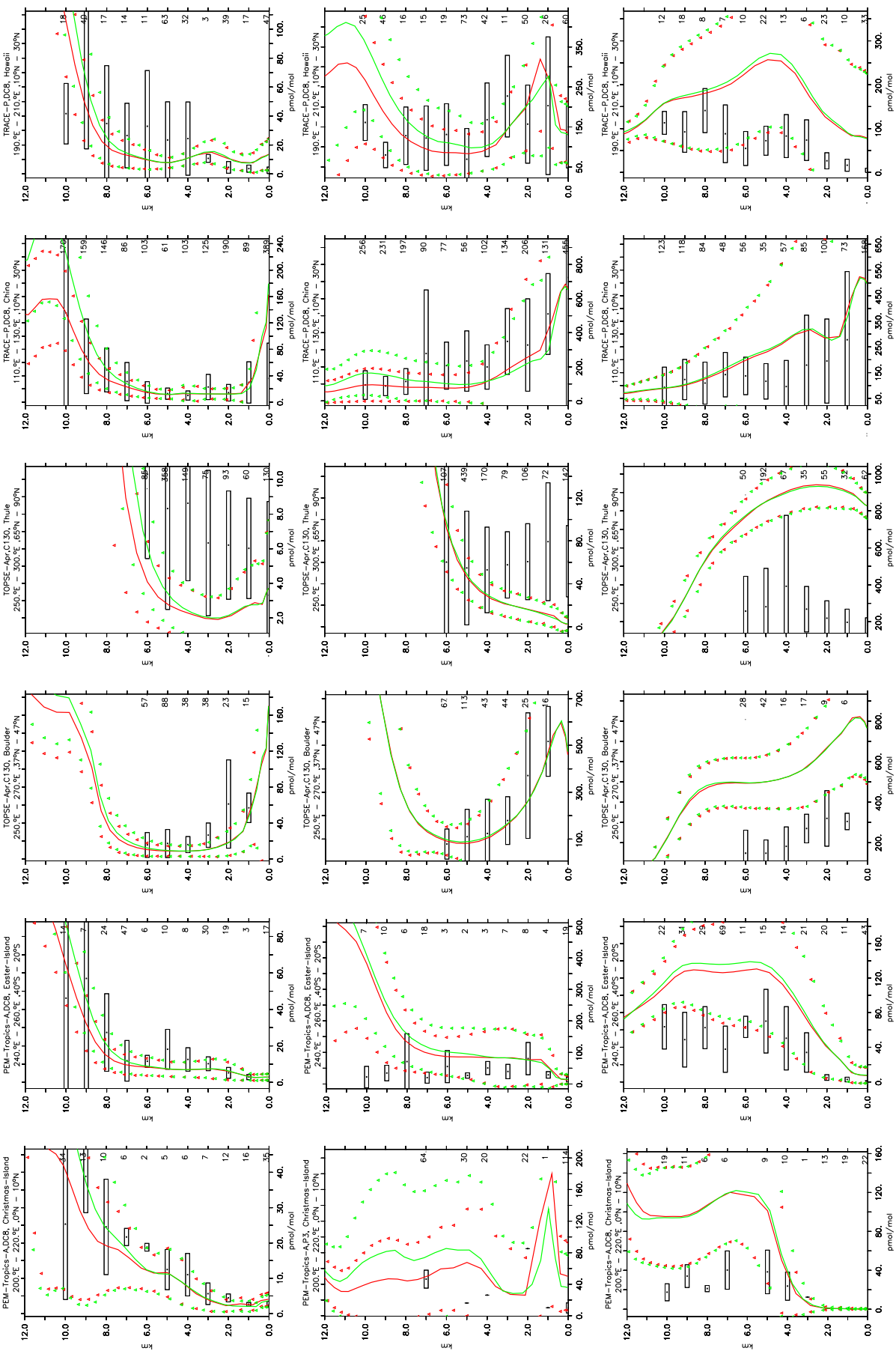

Figure 15: Profiles (in pmol/mol) of NO (top, filtered for daytime values, see text of Jöckel et al. (2006)), HNO_3 (middle) and PAN (bottom) for the simulated year 2000 (S1: red; S-new: blue) compared to composite data for selected regions from Emmons et al. (2000).

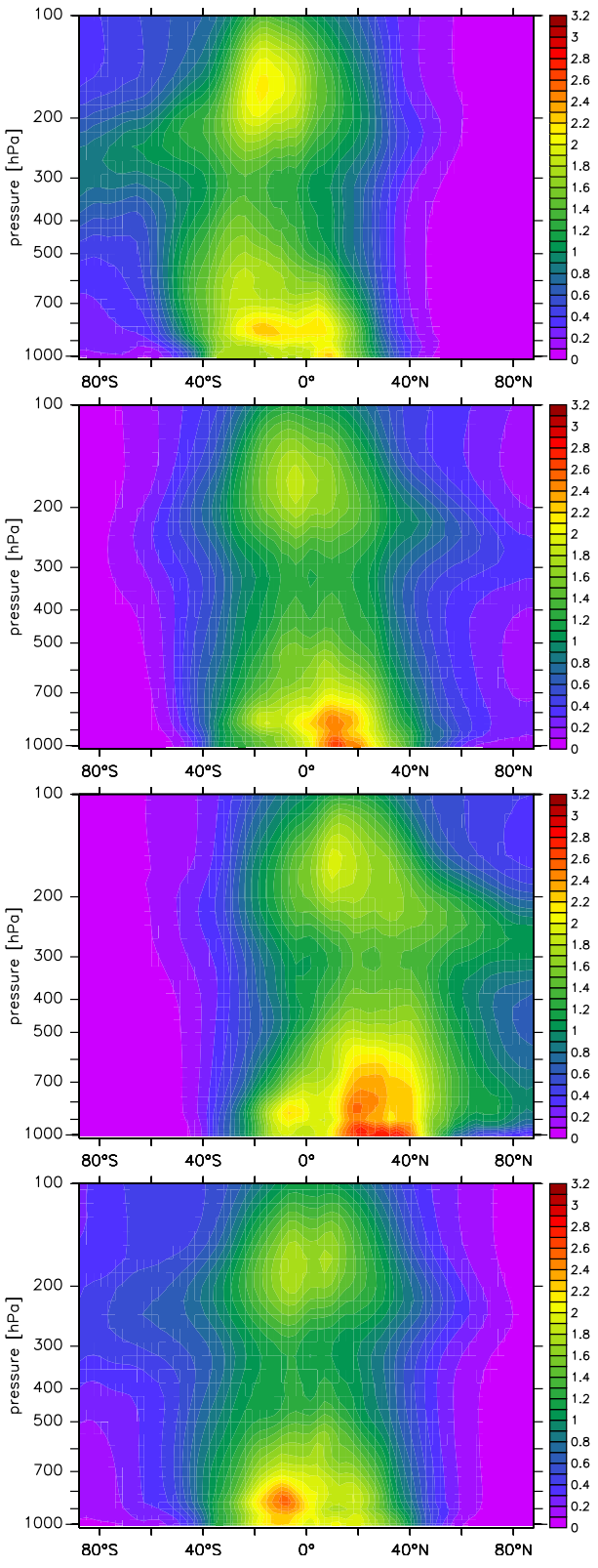

Figure 17: 1-yr average (2000) of simulated (S-new) zonal and diurnal mean OH (10^6cm^{-3}) for all seasons (DJF: first row; MAM: second row; JJA: third row; SON: last row).

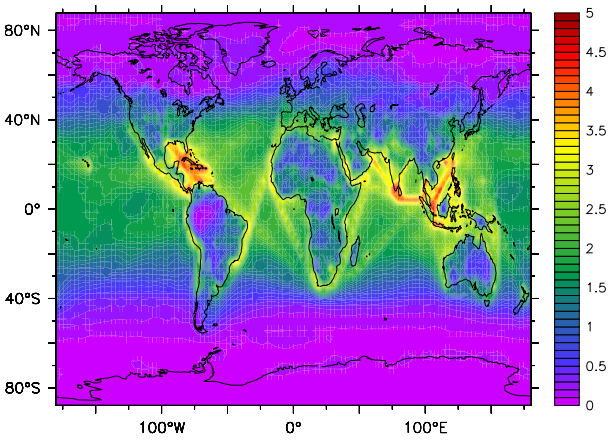

Figure 16: 1-year average (2000) of simulated (S-new) diurnal mean OH (10^6cm^{-3}) in the lowest model layer.

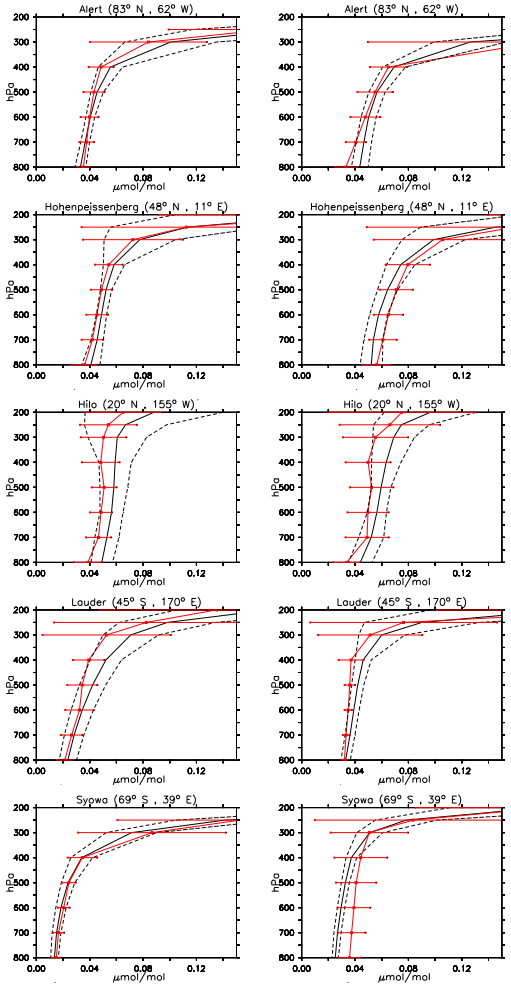

Figure 18: Vertical profiles of ozone (in µmol/mol) in January (left) and June (right) in the free troposphere and tropopause region for selected sites from Logan (1999). Black lines are model results (3-year averages, S-new) and red lines are observations. The dashed black lines show the model standard deviations and the red bars the observed standard deviations.

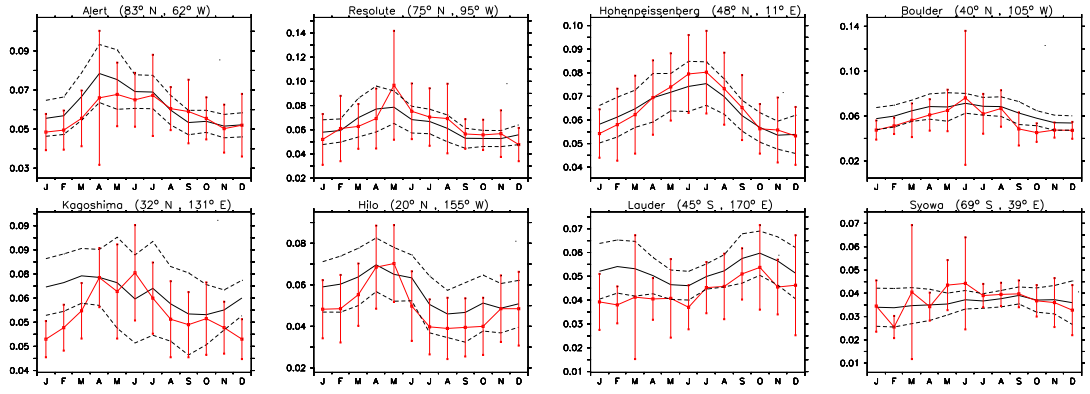

Figure 19: Seasonal cycle of ozone (in µmol/mol) for selected sites from Logan (1999) in the troposphere at 400 hPa. Black lines are model results (3-year averages, 1998-2000, S-new) and red lines are observations. The dashed black lines show the model standard deviations and the red bars the observed standard deviations.

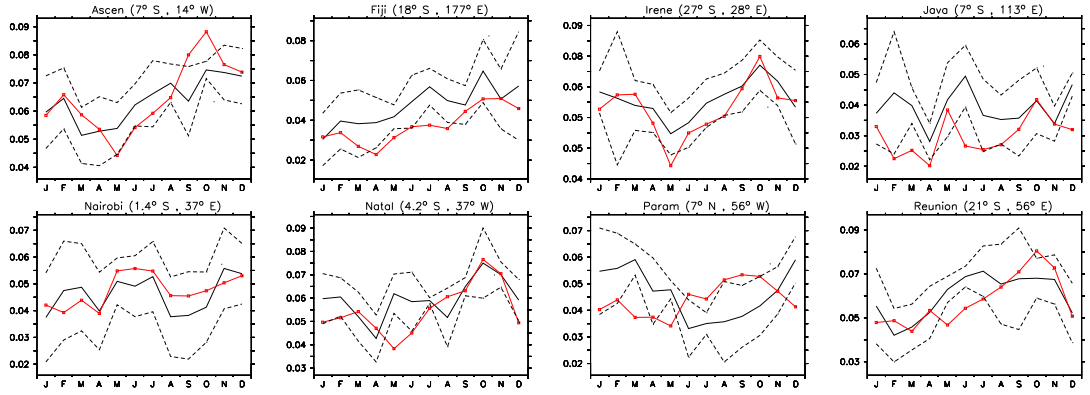

Figure 20: Seasonal cycle of ozone (in µmol/mol) at 412 hPa obtained from the SHADOZ database (red) compared to the 3-year climatology (1998-2000) derived from the E5/M1$^+$ model simulation S-new (black). The dashed black lines show the model standard deviations.

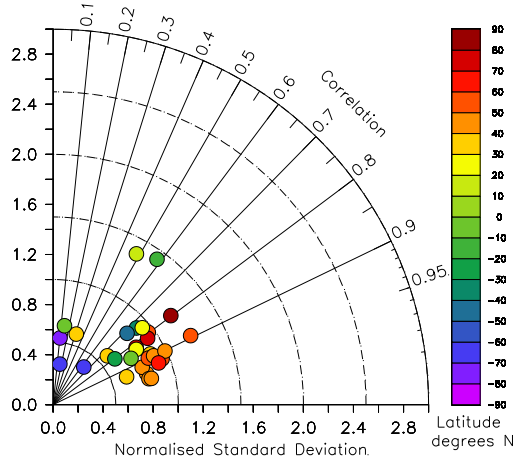

Figure 21: Taylor plot of the correlation between observations and model results (S-new) for the 400 hPa level for all sites from Logan (1999). The correlations has been error weighted. For a detailed explanation of the Taylor plots see Appendix D of Jöckel et al. (2006).

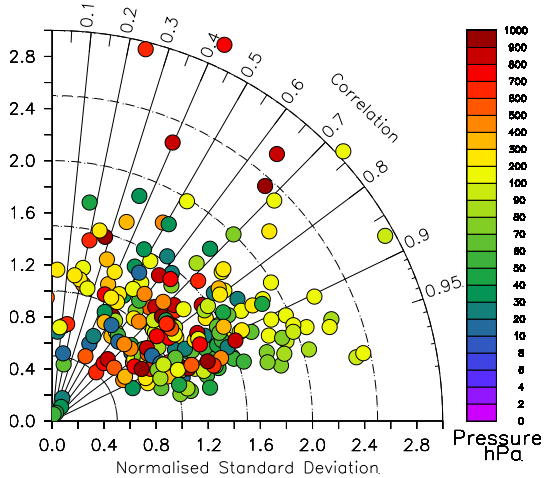

Figure 22: Taylor plot of O_3 correlation between 3-year E5/M1$^+$ climatology (S-new) and a similar climatology compiled from the SHADOZ database, see Sect. 5.4 of Jöckel et al. (2006).

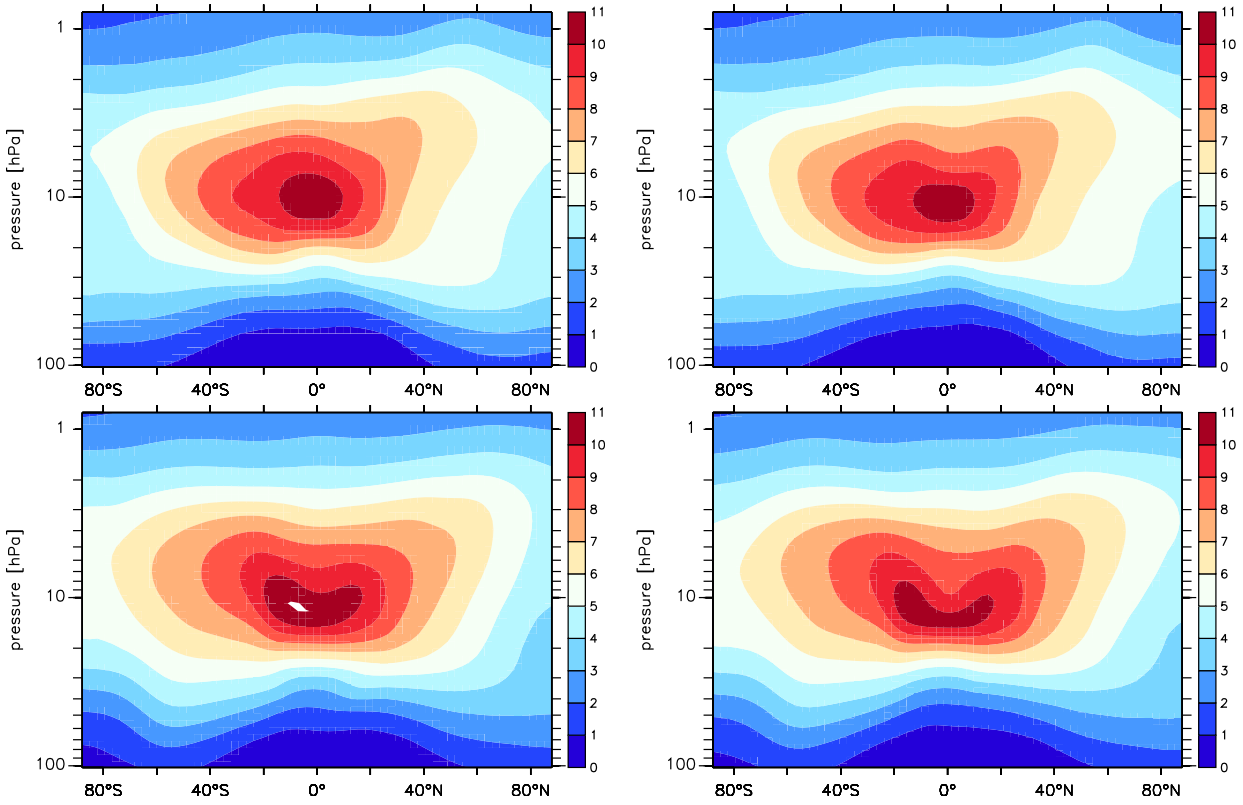

Figure 23: Zonal averages of simulated ozone (in µmol/mol). Top: DJF, bottom: SON; left: S-new; right: S1.

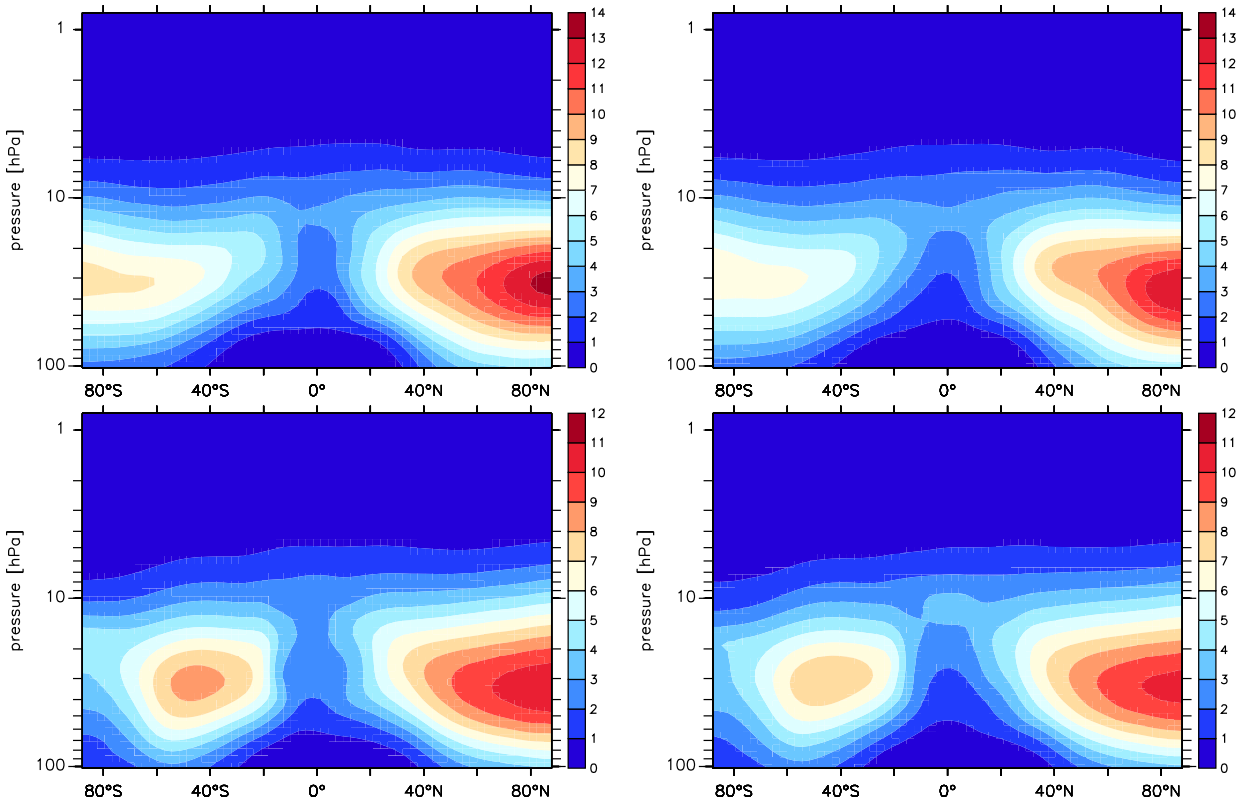

Figure 24: Zonal averages of simulated HNO_3 (in nmol/mol). Top: DJF; bottom: SON; left: S-new; right: S1.

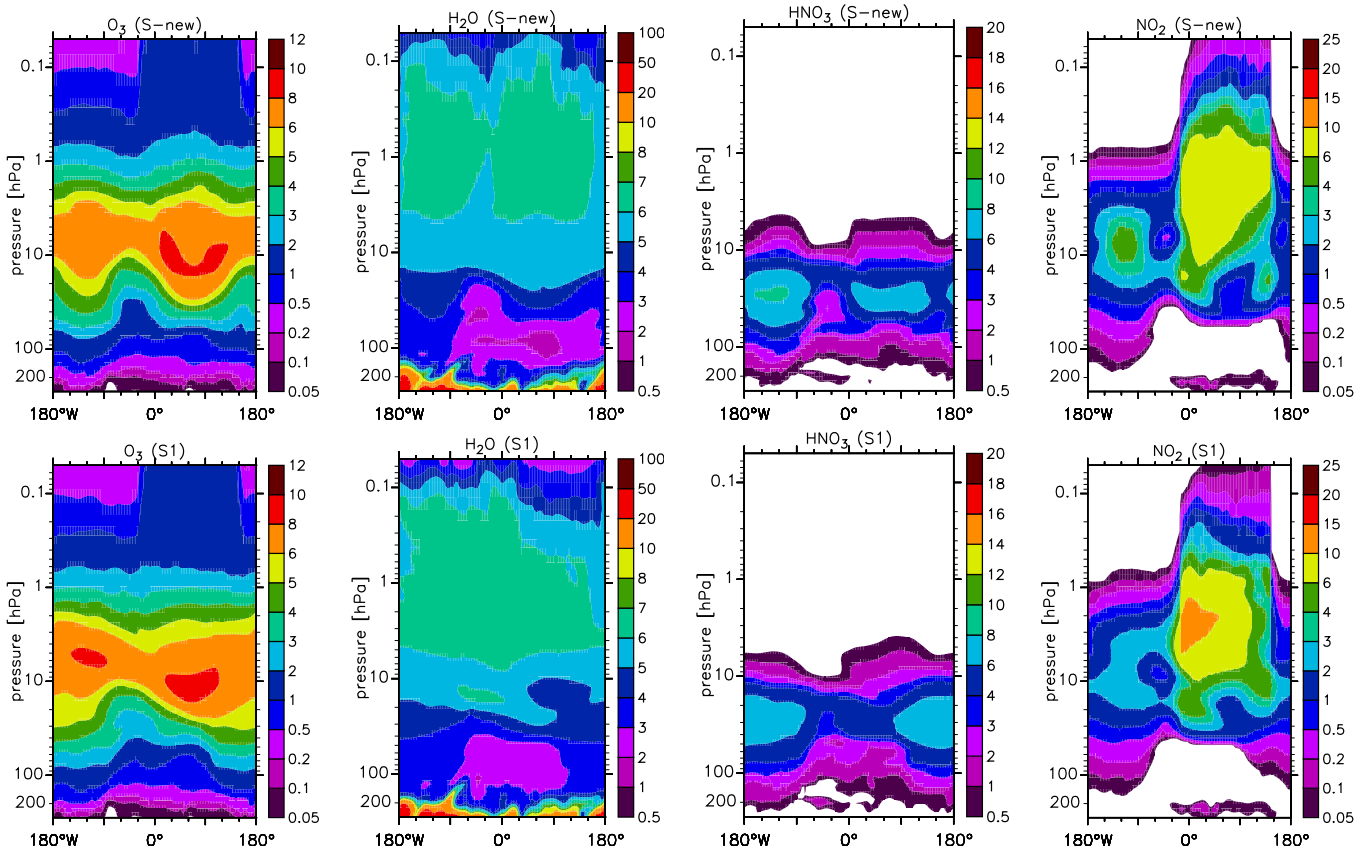

Figure 25: Model simulations (S-new, S1) of ozone (µmol/mol), water vapour (µmol/mol), HNO_3 (nmol/mol) and NO_2 (nmol/mol) for 22 September 2000, at 63° S.

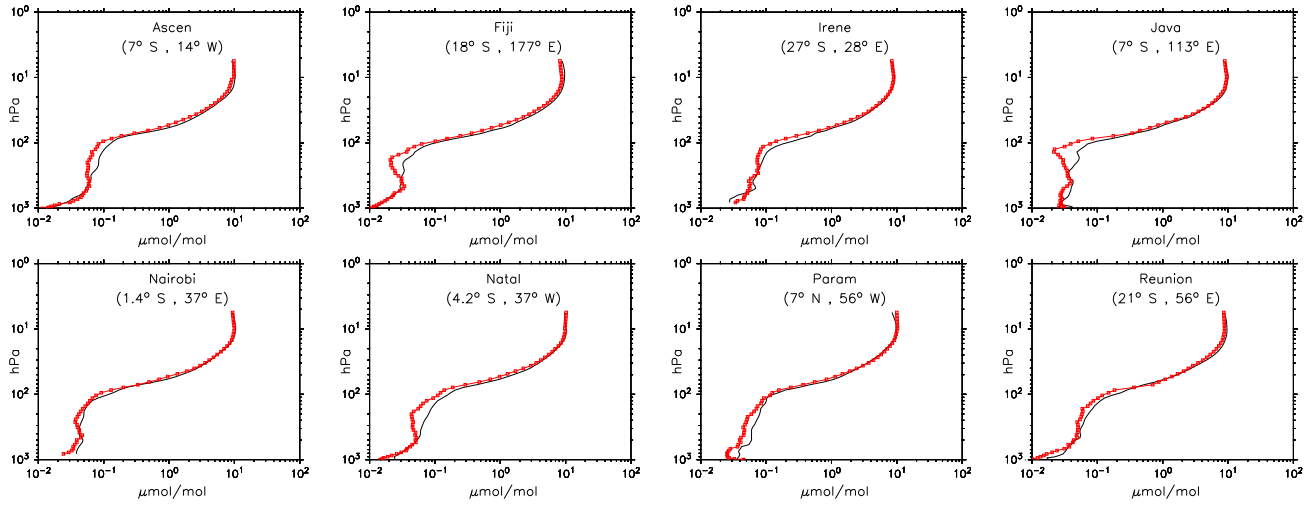

Figure 27: Vertical profiles of ozone (in µmol/mol) for January for the sites from the SHADOZ database. Model climatology (S-new) in black and measured climatology in red.

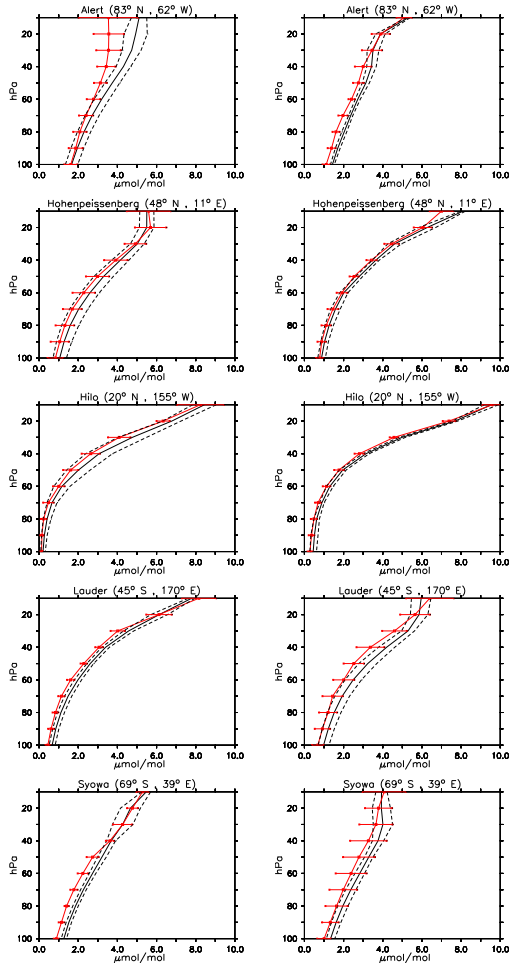

Figure 26: Observed and simulated (S-new) vertical profiles of ozone (in µmol/mol) for January (left) and June (right) in the free stratosphere for selected sites from Logan (1999). Colours and line styles as in Fig. 18.

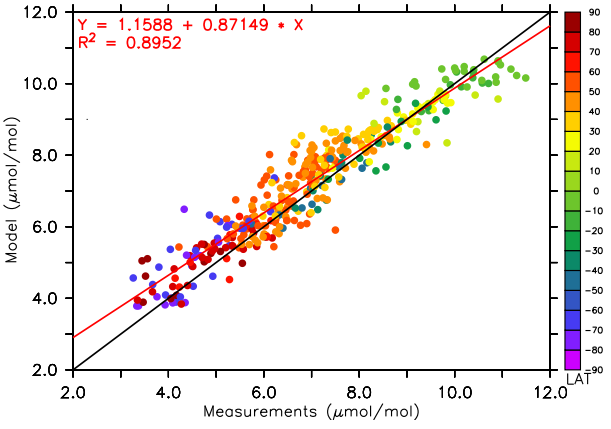

Figure 28: Comparison of simulated (E5/M1$^+$, S-new) and observed (Logan, 1999) vertical maximum O_3 mixing ratio (in µmol/mol). The colour code denotes the latitude.

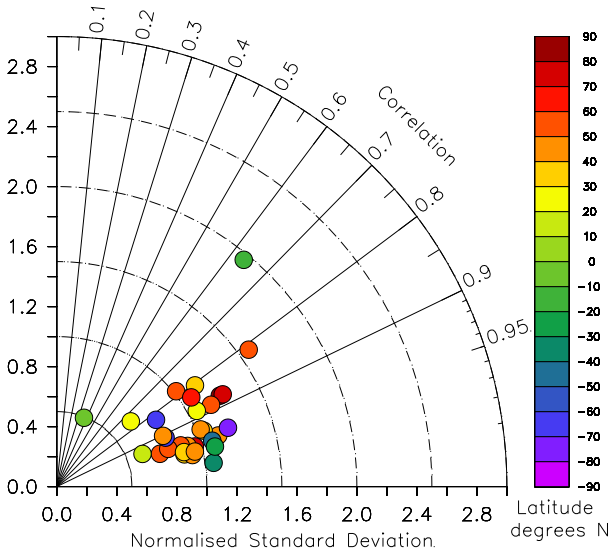

Figure 30: Taylor plot of the correlation between observations and model results (S-new) for the 40 hPa level for all sites from Logan (1999). The correlation has been error weighted (For a detailed explanation of the Taylor plots see Appendix D of Jöckel et al. (2006)).

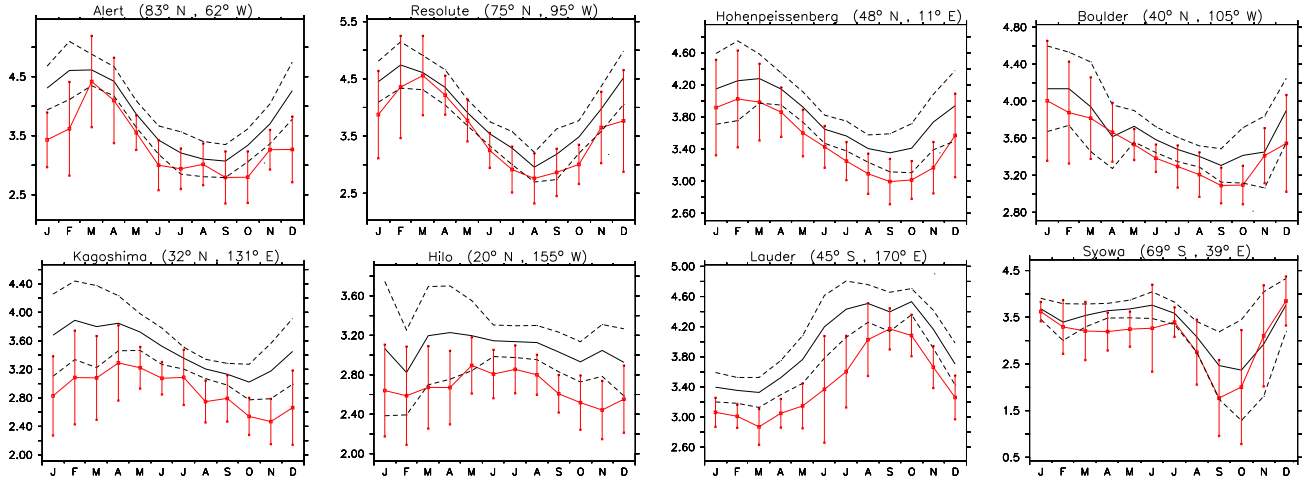

Figure 29: Seasonal cycle of ozone (in µmol/mol) for selected sites from Logan (1999) in the stratosphere at 40 hPa. The model results (S-new, black) represent a 3-year average (1998-2000).

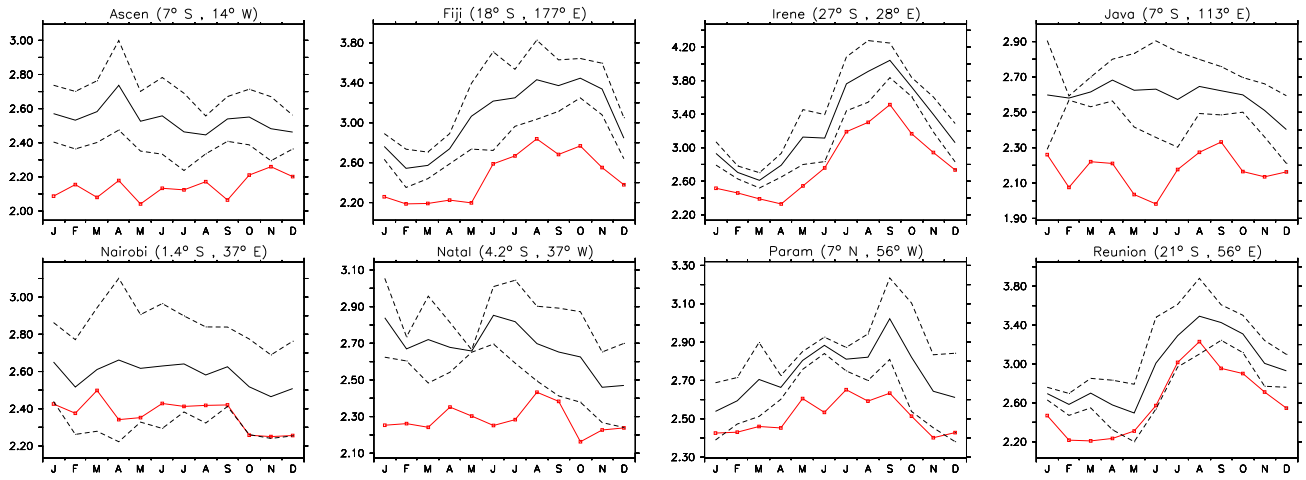

Figure 31: Seasonal cycle of ozone (in µmol/mol) at 40 hPa obtained from the SHADOZ database (red) compared to the 3-year climatology (1998-2000) derived from the E5/M1$^+$ model simulation S-new (black).